

Photodissociation of methylazide: Observation of triplet methylnitrene radical

Liming Ying, Yu Xia, Hairong Shang, Xinsheng Zhao,^{a)} and Youqi Tang

Department of Chemistry and Institute of Physical Chemistry, Peking University, Beijing 100871, China

(Received 24 April 1996; accepted 1 July 1996)

An investigation of the photodissociation of methylazide at wavelengths from 292 nm to 325 nm is presented. Emission spectra and lifetime analysis show the existence of the triplet CH_3N radical. A simple kinetic model is proposed to explain the observed fluorescence real time profile, which reflects the vibrational relaxation of hot radical at high pressures. The photodissociation dynamics of methylazide seems complex. The predominant channel is likely to produce CH_2NH via concerted 1,2-hydrogen shift and N_2 extrusion process. The triplet CH_3N comes from a minor spin-forbidden channel which involves possibly strong interaction between the low-lying excited singlet and triplet states of methylazide. © 1996 American Institute of Physics. [S0021-9606(96)00138-9]

I. INTRODUCTION

Azides and nitrenes play significant roles in organic reactions,¹ among them both methylazide and methylnitrene are their simplest alkyl-substitute forms. From 1950's to 1980's, people made a great effort to obtain the methylnitrene radical through photodissociation of methylazide in gas phase and matrix,²⁻⁵ however, only the isomer methyleneimine (CH_2NH) was observed. Bock *et al.*^{6,7} obtained a similar result in pyrolysis of methylazide more recently. It was generally accepted that the intermediate singlet methylnitrene is unstable and easily rearranges to methyleneimine as soon as it is produced.^{8,9}

The isomerization of both triplet and singlet methylnitrene to methyleneimine have been the subject of several *ab initio* calculations. Demuyck *et al.*¹⁰ and later Pople *et al.*¹¹ found that although the triplet ground state has a significant activation barrier to the 1,2-hydrogen shift, there appears to be no such barrier separating the 1E state from ground state methyleneimine. Nguyen⁹ held that singlet methylnitrene may be an evanescent intermediate in the photochemical decomposition of methylazide. He also noted that both experimental and *ab initio* investigations showed that methylnitrene does not rearrange via the 1,2-hydrogen shift to methyleneimine in its triplet ground state, suggesting that the direct photolysis of methylazide yielding methyleneimine proceeds via a singlet excited state.^{8,9} This hypothesis is consistent with the general opinion that hydrogen migration tends to occur on the singlet potential energy surface.^{8,12} More recently, Richards *et al.*⁸ re-examined the rearrangement of methylnitrene to methyleneimine on the lowest-lying singlet surface using CISD levels of theory. They found that the conclusion of most previous lower level studies that there is no barrier to rearrangement on the $^1A'$ surface appears to be justified.

The triplet methylnitrene is stable and faces a large barrier to unimolecular rearrangement as predicted by several *ab initio* calculations.⁸⁻¹¹ The first experimental evidence for its

existence was provided by the ESR spectra of Wasserman *et al.* in 1964.¹³ The definite observation of the triplet methylnitrene radical was made by Carrick and Engelking who obtained its $\tilde{A}^3E \rightarrow \tilde{X}^3A_2$ ultraviolet emission spectrum in 1984.¹⁴ The geometry of ground state methylnitrene was determined by high-resolution gas-phase emission spectroscopy.¹⁵ The vibrational frequencies for the ground and excited states have been derived from the jet-cooled UV emission spectra¹⁶ and the absorption spectra of matrix isolated methylnitrene.¹⁷ More recently, the laser induced fluorescence spectra of triplet methylnitrene have been reported.^{18,19,20} The lifetimes of several vibrational \tilde{A}^3E states have been measured, and showed that the \tilde{A}^3E state is bound at least up to 4800 cm^{-1} and is relatively free from photochemistry.²⁰

Recently, the isoelectronic diradical, methylcarbene, has been of great interest to theoreticians²¹⁻²⁵ as well as experimentalists.²⁶ Different from methylnitrene, singlet methylcarbene is a true intermediate that exists in a potential energy minimum and has a finite lifetime.^{21,25,26} The most recent *ab initio* investigation gave the activation barrier 1.2 kcal mol^{-1} for the isomerization of singlet methylcarbene to ethylene.²⁵ The lifetime of methylcarbene in pentane at ambient temperature was determined to be 0.5 ns and the activation barrier was estimated to be less than 2.3 kcal mol^{-1} experimentally.²⁶ Through comparison with methylcarbene, it seems even more difficult to observe singlet methylnitrene in decomposition of methylazide.

Because methylazide and hydrazoic acid (HN_3) all have an azide group as their chromophore, they have similar electronic structure for the first few electronic states and thus give similar UV absorption spectra consisting of two bands; one near 287 nm arising from $n \rightarrow \pi^*$ transition, and the other near 216 nm from $\pi \rightarrow \pi^*$ transition.²⁷ The dissociation dynamics of methylazide on the first excited singlet surface was studied experimentally via resonance Raman spectroscopy.²⁸ A dissociation process of concerted N_2 elimi-

^{a)} Author to whom correspondence should be addressed.

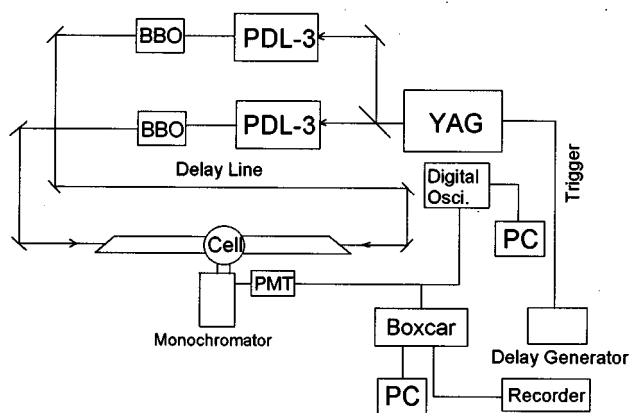


FIG. 1. Experimental setup for the photodissociation of CH_3N_3 . The second dye laser and the optical delay line were used in photolysis-probe experiments.

nation and 1,2-hydrogen shift has been proposed. However, the dissociation dynamics of methylazide in its first absorption band may be more complex. Our recent investigation of the photodissociation of methylazide at wavelengths from 292 nm to 315 nm has shown that the triplet methylnitrene can be produced.²⁹ Two-color photolysis-probe experiments has justified the existence of triplet methylnitrene radical in photodissociation of methylazide. The spectral and lifetime evidences will be provided and the dissociation mechanism will be proposed.

II. EXPERIMENT

Methylazide was prepared by the reaction of dimethyl sulfate and sodium azide.¹⁴ The experimental setup is shown in Fig. 1. The photodissociation of methylazide was investigated in the UV region from 292 nm to 325 nm in a flowing gas cell. This wavelength region locates at the long wavelength side of the first electronic absorption band ($n \rightarrow \pi^*$) of methylazide. The sample pressure was monitored by a Baratron (MKS) and was maintained typically at 30 Torr. The sample was kept refreshed after each laser shot. The visible beam was produced by a PDL-3 dye laser pumped by the second harmonic of a GCR-4 YAG laser (Spectra Physics) with pulse duration of 6 ns and repetition rate of 30 Hz. R610, R640, and DCM dyes (Exiton) were used. The visible output was frequency doubled in a BBO (Cstech) crystal to cover the desired wavelengths. UV beam went into the cell through a quartz window with Brewster angle to reduce the laser scattering light. A 300 mm focal-length convex lens was used to focus the laser beam. Side emissions were collected by a set of focus lenses and dispersed by a monochromator (WDP500-2A, the Second Optical Factory of Beijing) with a 1200 grooves/mm grating. The output of the R955 photomultiplier (Hamamatsu) was preamplified by an SRS445 preamplifier (Stanford Research) and averaged by a 4100 Boxcar system (EG&G). The digital data were transferred to a 286 computer via GPIB bus. The analog data were

transferred to a recorder to record the spectra simultaneously. In lifetime measurements, an HP54510A digital oscilloscope (Hewlett-Packard) was employed to digitizing the real-time signal, and the data were transferred to a 386SX/25 computer via GPIB bus.

In further two-color photolysis-probe experiments, the pumping laser was separated into two beams by a beamsplitter. Two 532 nm laser beams pumped two PDL-3 dye lasers respectively. The outputs were both frequency doubled in BBO crystals. Two 300 mm focal-length convex lenses were used to focus the laser beams. The probe beam spatially overlapped with the photolysis beam in the cell center with an optical delay of 26 ns. The focus spot size of the probe beam was smaller than that of the photolysis beam. Laser energies were measured by a power meter (Scientech). The detection and data processing part was the same as that of one-color experiments described above.

III. RESULTS AND ANALYSIS

A. Emission spectra in photolysis of methylazide

The emission spectra were obtained at different photolysis wavelengths ranged from 292 nm to 325 nm. Because the first excited state of methylazide is dissociative, the pure-dephasing rate will be much slower than the total dephasing rate. Thus, the emission spectra of methylazide was expected to behave as resonance Raman.³⁰ However, more complex emission spectra were observed. Some emission features track with the photolysis laser wavelengths and are Raman-type, while others fix at definite emission wavelengths and are fluorescencelike. The Raman-type emissions come from the dissociating methylazide molecule and are assigned to the resonance Raman emissions reflecting the photodissociation dynamics of methylazide which is a process of concerted N_2 extrusion and 1,2-hydrogen shift, as studied previously.²⁸ The fluorescencelike emissions have definite lifetimes.

Two ways may contribute to the fluorescence emissions; the interference of impurities and the fluorescence of photodissociation products. Since GC-MS analysis of the synthesized methylazide sample showed that the main impurity is methanol, a comparison experiment was done using pure methanol instead of methylazide in the same condition. O-H stretch vibration frequency was observed at about 3700 cm^{-1} Raman shift, while no fluorescence emission was found. Although strong Raman lines were found at about 2900 cm^{-1} in both cases of methylazide and methanol, no distinguishable peak appeared at 3700 cm^{-1} for methylazide. Therefore, the interference of methanol impurity in Raman and fluorescence spectra can be excluded. The primary photodissociation product of methylazide is methyleneimine (CH_2NH) as reported already.²⁻⁵ No electronic spectrum of methyleneimine has been found experimentally in literature. The theoretically predicted value for the vertical excitation for the lowest singlet state in CH_2NH is 5.45 eV (Ref. 31) which is much higher than our observed emission bands. Therefore, there exist few possibilities that the fluorescence comes from CH_2NH . Based on our previous laser spectroscopy

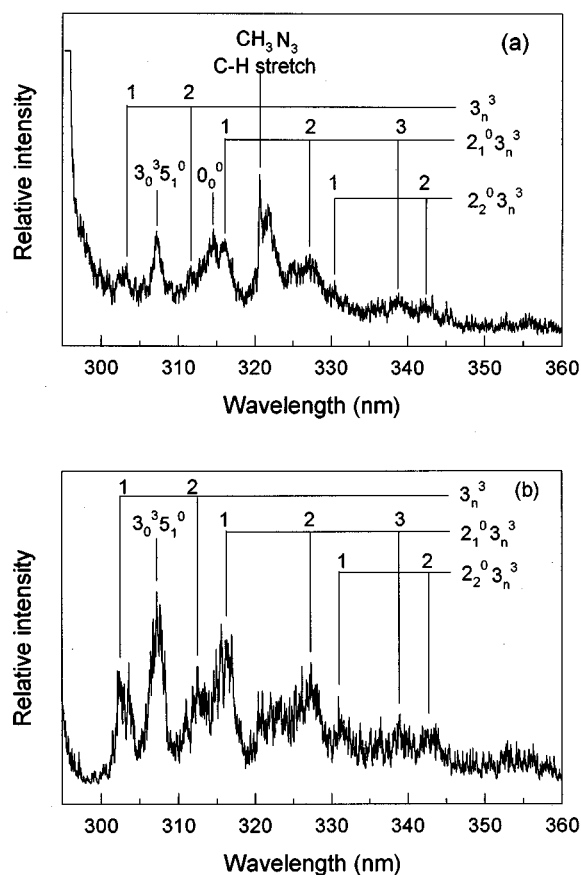


FIG. 2. Comparison of the laser induced emission spectra showing the existence of the triplet CH_3N radical. The laser wavelength is 294 nm, corresponding to the excitation of the 3_0^3 band of the $\tilde{A}^3E \leftarrow \tilde{X}^3A_2$ transition of CH_3N . (a) Produced in the photolysis of CH_3N_3 ; (b) produced in the reaction of CH_3N_3 with metastable N_2 (Ref. 20).

study on the methylnitrene radical²⁰ and the spectra data of the $\tilde{E}^3E \rightarrow \tilde{X}^3A_2$ emission,¹⁶ the fluorescence part of the emission can be assigned to the emission of triplet excited methylnitrene radical. Other evidences such as excitation spectra and lifetime also support the assignment of the fluorescence emission from the \tilde{A}^3E state CH_3N radical.

Figure 2(a) shows the emission spectrum in the photodissociation of methylazide at 294 nm which also exactly matches the excitation of the 3_0^3 band of the $\tilde{A}^3E \leftarrow \tilde{X}^3A_2$ transition of CH_3N . Figure 2(b) is the dispersed fluorescence spectrum of the 3^3 band obtained previously in our LIF study of the CH_3N radical produced by the reaction of CH_3N_3 with metastable N_2 .²⁰ It can be seen clearly that the fluorescence part of Fig. 2(a) fits the pure fluorescence spectrum of Fig. 2(b) very well in both the position and relative intensity of the peaks, indicating that the ground state CH_3N is present in the photolysis product and is excited by the same photolysis laser. If the photolysis wavelength deviated from the electronic absorption band of the CH_3N radical, emissions from the excited CH_3N can still be seen though the intensity is weaker. These observations show that both the excited and ground state CH_3N radical exist in photodissociation of methylazide.

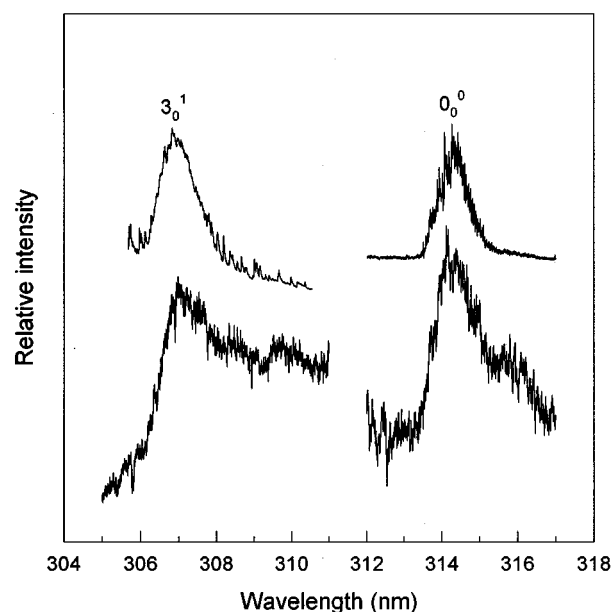


FIG. 3. Fluorescence excitation spectra of the triplet CH_3N radical. Upper spectrum: Radical produced in the reaction of CH_3N_3 with metastable N_2 (Ref. 20). Lower spectrum: Radical produced in the photolysis of CH_3N_3 .

B. Excitation spectra

The excitation spectra were obtained when the photolysis laser was scanned while the monochromator with a resolution of 3 nm was set at 325 nm and 328 nm, corresponding to collect the fluorescence of the 0^0 band and the 3^1 band of the $\tilde{A} \rightarrow \tilde{X}$ system of CH_3N , respectively. As shown in Fig. 3, the distinct peaks at about 314 nm and 307 nm fit well to our previously reported fluorescence excitation spectrum.²⁰ But in the lower spectrum, some shoulders can be found, especially for the origin band. The excitation of vibrationally hot radicals may be responsible for this. In our previous experiments, the CH_3N radical was produced by the collisional reaction of metastable N_2 with CH_3N_3 . The detection zone was 4 cm downstream the reaction zone. Therefore, although the hot radicals may be produced by the reaction, they almost relax to the vibrationless state; whereas in photolysis, vibrational relaxation will not be so complete within the laser pulse even though the pressure is rather high. The shoulder appears near 316 nm is assigned to the 6_1^1 band, in agreement with the earlier observation of Carrick and Engelking.¹⁴

C. Lifetime simulation and the kinetic model

The fluorescence decay profiles of the 0^0 band and the 3^1 band were recorded at various pressures. Only the fluorescences at the range of 325 ± 3 nm and 328 ± 3 nm, respectively, were collected by the monochromator. The time profiles were simulated by the method of least-squares fit.³² Because the laser pulsewidth in the experimental condition is

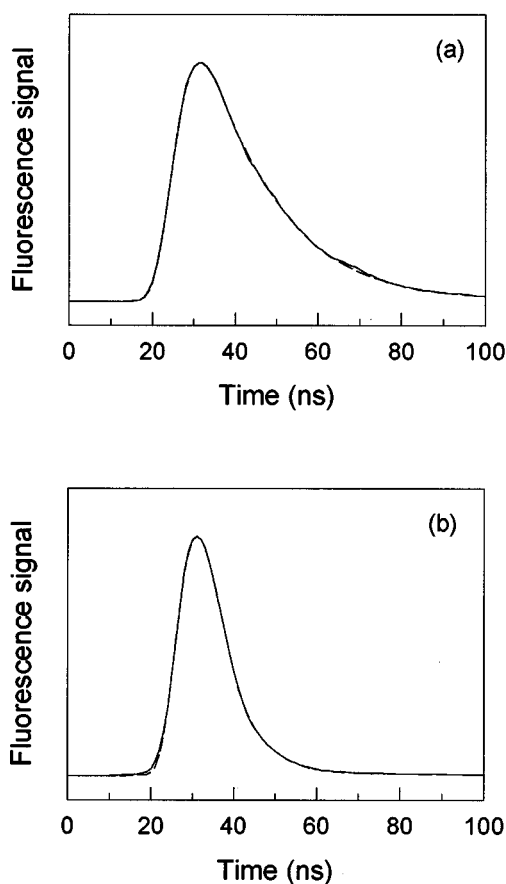


FIG. 4. Fluorescence time profiles of the \tilde{A} -state CH_3N radical. (a) Radical in the ground vibration state at a pressure of 25.9 Torr; (b) radical in the $v_3' = 1$ state at a pressure of 23.1 Torr. Dashed line, simulated; solid line, experiment.

not negligible, a convolution method was used. The measured fluorescence real-time profile was simulated by the convolution of the real-time profile of laser scattering light with the monoexponential decay of the fluorescence. The contribution of the background fluorescence or Raman signals were considered when necessary. It should be noted that the photolysis of CH_3N_3 and the excitation of methylnitrene were achieved by the same laser beam. As a result, the simulation method described here is approximate. The examples of experimental and simulated fluorescence time profiles of excited CH_3N in ground vibration state at different pressures are presented in Figs. 4 and 5. The extrapolated radiative lifetimes of the ground and $v_3' = 1$ \tilde{A} -states are 500 ns and 460 ns, respectively, as shown in Fig. 6. These values are not very accurate because of high pressure, yet they are consistent with our latest detailed lifetime measurement, which are 413 ± 12 ns and 374 ± 20 ns for the ground and $v_3' = 1$ \tilde{A} -states,³³ where CH_3N was generated by standard discharge method.²⁰ The quenching rates of the CH_3N radical by bulk CH_3N_3 were obtained from the plots of the decay rate vs pressure, which are $0.80 \times 10^{-10} \text{ cm}^3 \text{ s}^{-1} \text{ molecule}^{-1}$ and $2.2 \times 10^{-10} \text{ cm}^3 \text{ s}^{-1} \text{ molecule}^{-1}$ for the ground and $v_3' = 1$ vi-

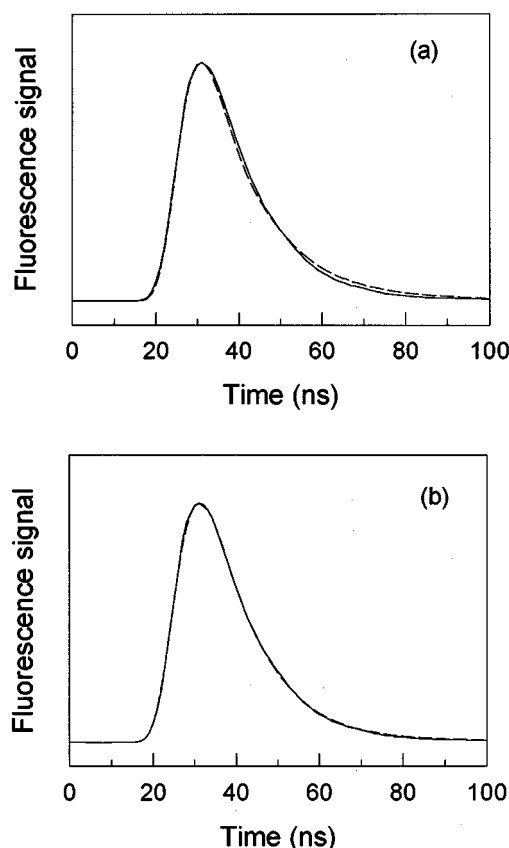


FIG. 5. Fluorescence time profiles of the \tilde{A} -state CH_3N radical in the ground vibration state at a pressure of 44.9 Torr. (a) Simulated by one component exponential decay; (b) simulated by Eq. (1). Dashed line, simulated; solid line, experiment.

bration state, respectively. The relatively large difference between them is probably brought by the additional vibrational relaxation of the vibrationally excited state.

It was found that the simulation curve does not fit the experimental curve at high pressure as shown in Fig. 5. However, if the simulation was carried out by following equation:

$$F(t) = e^{-(t-t_0)/\tau_1} - B e^{-(t-t_0)/\tau_2}, \quad (1)$$

the simulated results can be greatly improved. A kinetic model for the photodissociation of CH_3N_3 demonstrated in Fig. 7 was proposed to explain the above phenomenon. In the photolysis both ground and excited vibrational \tilde{A}^3E states were produced. At high pressure, the vibrational relaxation should not be neglected, the vibrationally excited radicals may relax to the ground state before they emit fluorescence. Because the existence of the parallel reaction channel of k_8 , the lifetime of CH_3N_3^* is very short.²⁸ The production of the primary products can be considered to be instantaneous as soon as the molecule absorbs photons for the purpose of simulation. In other words, k_4, k_5, k_6, k_7, k_8 only come in as factors affecting the branching ratio, while for time evolution, we only need consider convolution of the laser pulse and the following rate equations:

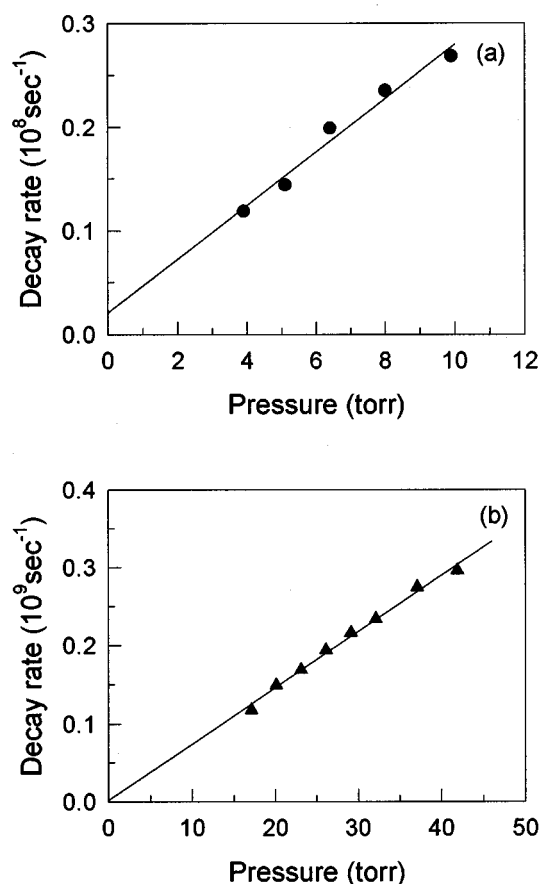


FIG. 6. Fluorescence decay rates vs total pressure of the \tilde{A} -state CH_3N radical in ground vibrational and $v_3' = 1$ states. (a) $v_3' = 0$; (b) $v_3' = 1$.

$$\frac{d[\text{CH}_3\text{N}^*(v=0)]}{dt} = -k_1[\text{CH}_3\text{N}^*(v=0)] + k_2[\text{CH}_3\text{N}^*(v \neq 0)], \quad (2)$$

$$\frac{d[\text{CH}_3\text{N}^*(v \neq 0)]}{dt} = -(k_2 + k_3)[\text{CH}_3\text{N}^*(v \neq 0)]. \quad (3)$$

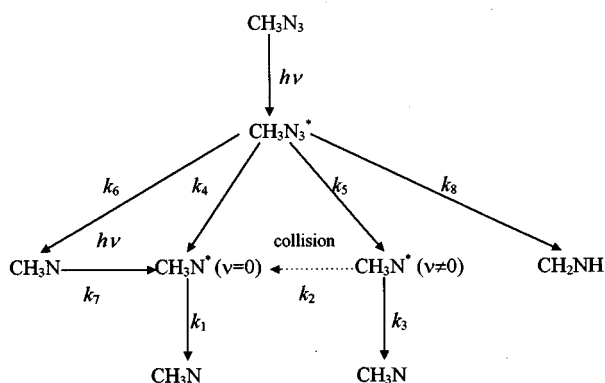


FIG. 7. Kinetic model for the photodissociation of CH_3N_3 .

TABLE I. Rate constants at different pressures.

Pressure (Torr)	k_1 (10^8 s^{-1})	$k_2 + k_3$ (10^8 s^{-1})
44.9	1.00	2.21
40.6	0.95	2.30
36.1	0.96	1.58
32.6	0.89	1.73
29.2	0.82	1.17
25.9	0.75	1.01
22.5	0.68	0.90

Provided that $[\text{CH}_3\text{N}^*(v=0)] = C_1$, $[\text{CH}_3\text{N}^*(v \neq 0)] = C_2$ initially, then

$$[\text{CH}_3\text{N}^*(v=0)] = \left(C_1 + \frac{C_2 k_2}{k_2 + k_3 - k_1} \right) e^{-k_1 t} - \frac{C_2 k_2}{k_2 + k_3 - k_1} e^{-(k_2 + k_3)t}. \quad (4)$$

Equation (4) can be simply written as

$$[\text{CH}_3\text{N}^*(v=0)] = A[e^{-k_1 t} - B e^{-(k_2 + k_3)t}]. \quad (5)$$

If $B \ll 1$, the second term of Eq. (5) can be neglected and the fluorescence decay is monoexponential. In general cases, the fluorescence decay is biexponential. Equation (5) is in agreement with Eq. (1) given above. Therefore, the rate constants k_1 , $k_2 + k_3$ can be derived from the lifetime simulation, and the results are presented in Table I. The relative values among k_1 and $k_2 + k_3$ agree with physical intuition.

D. Results and analysis of photolysis-probe experiments

The two-color photolysis-probe scheme was used to confirm the formation of the triplet CH_3N radical and to eliminate the interference of Raman signals in photodissociation of CH_3N_3 . A typical real-time emission curve is shown in Fig. 8 which clearly indicates the excitation of the ground state radical. The dispersed fluorescence spectrum of the origin band of CH_3N is presented in Fig. 9. This spectrum has a higher signal to noise ratio than that obtained from the one-color experiment. The emission bands and intensities are essentially the same as observed previously.²⁰ Although we made a great effort to prolong the optical delay between photolysis laser and probe laser, the value of 26 ns seems insufficient to avoid the strong photolysis laser scattering light. Thus the photolysis laser line still appears in the spectrum. Figures 8 and 9 firmly demonstrate the existence of the triplet CH_3N radical.

The $\tilde{A} \rightarrow \tilde{X}$ transition produces a large change in molecular geometry. In emission to the ground electronic state, the C-N bond tightens and the methyl group closes, which results in extensive progressions in the ν_3 mode (C-N stretch), and activates ν_1 and ν_2 modes, (the hydrogen stretch and the symmetric bend).¹⁶ The dispersed spectrum of the 3^1 band is shown in Fig. 10 which has not been reported yet. The spectrum mainly contains two progressions, namely 3_n^1 and $2_n^0 3_n^1$. The 3_n^1 band mixes with the 6_n^1 band because of the Jahn-

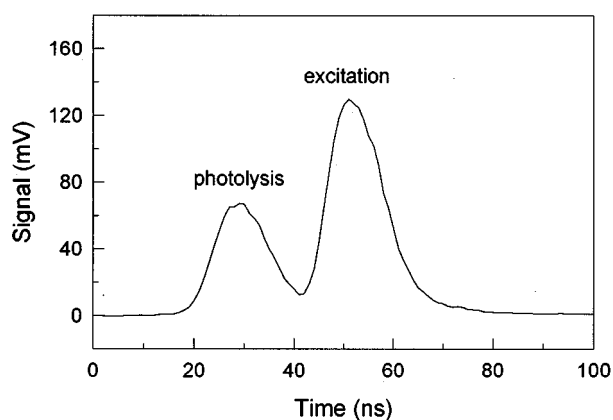


FIG. 8. Real-time emission signal in the photolysis-probe experiment at a total pressure of 42.4 Torr. The photolysis laser wavelength is 301.5 nm with an energy of 250 $\mu\text{J}/\text{pulse}$ and the probe laser wavelength is 314.29 nm with an energy of 50 $\mu\text{J}/\text{pulse}$. The monochromator is set at 324.9 nm with 1 nm resolution.

Teller effect in the degenerate \tilde{A}^3E state and the Fermi resonance, which will be discussed elsewhere.³³ Due to vibrational relaxation to the ground vibration state, fluorescence from the ground vibration state has also been observed, consistent with the kinetic model described above.

Since the excitation spectrum shows evidence of hot CH_3N radicals, the dispersed spectrum of the 6^1 band was obtained by 6_1^1 excitation at 315.88 nm after the photolysis of CH_3N_3 at 301.5 nm, as shown in Fig. 11. The methyl rocking vibration ν_6'' was first observed in emission spectrum.¹⁶ Its fundamental appears at 903 cm^{-1} . The ν_6'' mode also occurs in combination with the C–N stretch mode and in progressions from ν_6' in the excited state. The progression of 6_n^1 is

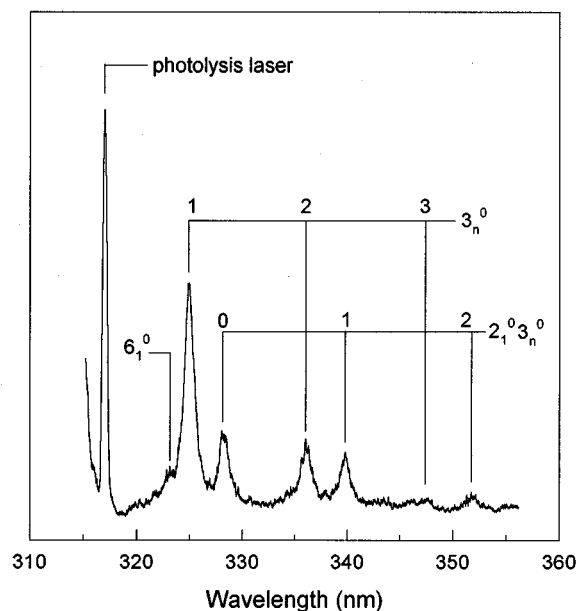


FIG. 9. Dispersed fluorescence spectrum of the origin band of CH_3N with 0.5 nm resolution in the photolysis-probe experiment after 0_0^0 excitation.

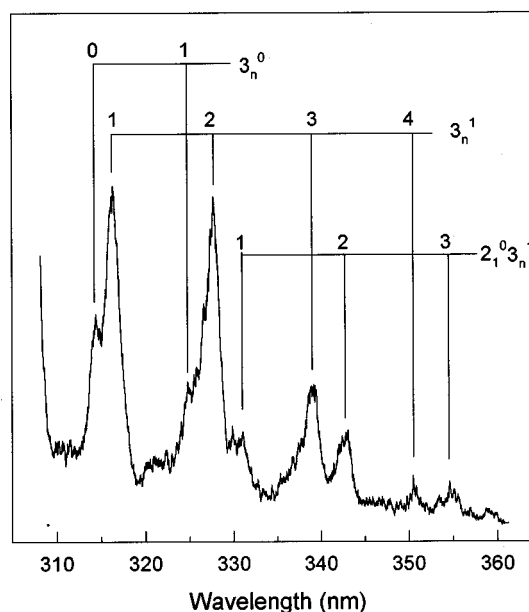


FIG. 10. Dispersed fluorescence spectrum of the 3^1 band of CH_3N with 1 nm resolution in the photolysis-probe experiment after 3_0^1 excitation.

observed in the dispersed LIF spectrum as expected. The combination progressions $2_1^0 6_n^1$, $3_1^0 6_n^1$, and $5_1^0 6_n^1$ are mixed with the main progression due to the low resolution of the spectrum.

IV. DISCUSSION

A. Is triplet CH_3N the direct photodissociation product of CH_3N_3 ?

The ground state of CH_3N_3 is singlet, so the most possible photodissociation process should occur on the first excited singlet potential surface. However, the triplet CH_3N radical is observed. Theoretical studies have shown that the rearrangement of the singlet CH_3N to CH_2NH via 1,2-

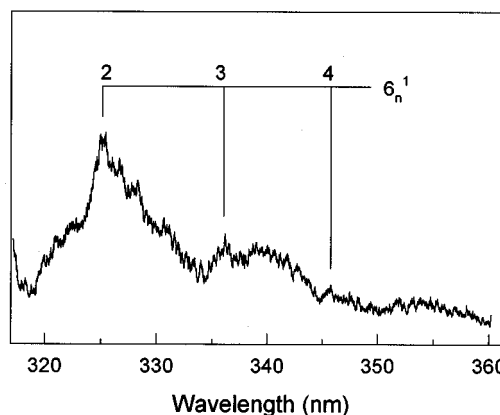


FIG. 11. Dispersed fluorescence spectrum of the 6^1 band of CH_3N with 1 nm resolution in the photolysis-probe experiment after 6_1^1 excitation.

hydrogen shift has no barrier,^{8–11} so the singlet CH₃N might be an evanescent intermediate or just a transition state on the potential surface. As a result, the singlet CH₃N radical has not been observed spectroscopically to date.

Collision-induced intersystem crossing might be responsible for the formation of triplet CH₃N after photodissociation of CH₃N₃. It was reported by Rohrer and Stuhl³⁴ that the collision-induced NH(*c*¹Π)→NH(*A*³Π) is very efficient with O₂, NO, and Xe, and excited NH(*A*³Π) radicals are noteworthy secondary products which can be generated in the HN₃ photolysis systems. But the estimated collision frequency in our experimental condition is one time per 2 ns, so there are few probabilities for singlet CH₃N to undergo intersystem crossing via a collision with precursor CH₃N₃ in the presence of a fast isomerization process due to the very short lifetime of singlet CH₃N if it does exist at all. In addition, as the primary product is CH₂NH, it is also not possible to produce triplet CH₃N via other secondary reactions. Therefore, the triplet CH₃N radical is most probably the direct photodissociation product of CH₃N₃.

B. Photodissociation dynamics of CH₃N₃

Because the formation of the triplet CH₃N radical is a spin-forbidden process, the interaction between the excited singlet and triplet states of CH₃N₃ might play a significant role in photodissociation. As the electronic structure of CH₃N₃ is similar to that of HN₃, it will be helpful to inspect the photodissociation of HN₃. The low-lying excited states of CH₃N₃ have not been theoretically investigated, only the UV absorption spectra were reported in solution.²⁷ On the contrary, the photolysis of HN₃ has been extensively studied experimentally and theoretically. Ground-state overtone pumped photolysis of HN₃(\tilde{X}^1A') involves a spin-forbidden dissociation channel HN₃(\tilde{X}^1A')→NH($\tilde{X}^3\Sigma^-$) + N₂($\tilde{X}^1\Sigma_g^+$), when overtone and combination levels of HN₃ in the range 5ν₁ to 6ν₁ are excited.³⁵ In the UV photodissociation of HN₃ at wavelengths of 248,³⁶ 266,^{37,38} 283,³⁹ and 308 nm,⁴⁰ the NH fragments are found exclusively in the *a*¹Δ state, while at 193 nm, all five low-lying states of NH are produced.³⁶ Recently, Alexander and Werner⁴¹ has proposed a reaction channel involving the crossing between the two dissociation pathways; HN₃(¹A'')→NH($\tilde{X}^3\Sigma^-$) + N₂($\tilde{X}^1\Sigma_g^+$), and HN₃(\tilde{X}^1A')→NH(*a*¹Δ) + N₂($\tilde{X}^1\Sigma_g^+$), to explain the formation of spin-forbidden product NH($\tilde{X}^3\Sigma^-$) in the dissociation of HN₃ by vibrational overtone pumping on the ground electronic surface. The vertical excitation energy for the lowest singlet excited state ¹A'' of HN₃ is 4.96 eV, and the lowest triplet state ³A'' is a little lower.⁴²

It might be reasonable to assume that there exists strong interaction between the low-lying excited singlet and triplet states of CH₃N₃, which leads to the formation of triplet CH₃N. There might be four reaction channels in the photodissociation of CH₃N₃, as shown in Table II. The enthalpies of reactions (i) and (iii) are obtained from our recent *ab initio* G2 (Ref. 43) calculation⁴⁴ using the GAUSSIAN 94 package of programs.⁴⁵ The calculated bond dissociation energy of

TABLE II. Relevant heat of reaction of methylazide.

Reaction channel	Δ <i>H</i> (kcal mol ⁻¹)
(i) CH ₃ N ₃ (\tilde{X}^1A') $\xrightarrow{h\nu}$ CH ₂ NH(\tilde{X}^1A') + N ₂ ($\tilde{X}^1\Sigma_g^+$)	-49.9
(ii) CH ₃ N ₃ (\tilde{X}^1A') $\xrightarrow{h\nu}$ CH ₂ NH(¹ A'') + N ₂ ($\tilde{X}^1\Sigma_g^+$)	20.0
(iii) CH ₃ N ₃ (\tilde{X}^1A') $\xrightarrow{h\nu}$ CH ₃ N(\tilde{X}^3A_2) + N ₂ ($\tilde{X}^1\Sigma_g^+$)	5.8
(iv) CH ₃ N ₃ (\tilde{X}^1A') $\xrightarrow{h\nu}$ CH ₃ N(\tilde{A}^3E) + N ₂ ($\tilde{X}^1\Sigma_g^+$)	96.6

CH₃N–N₂ is 39.8 kcal mol⁻¹, in agreement with the estimation value 40.6 kcal mol⁻¹ given by Bock and Dammel.⁷ The enthalpy of reaction (iv) is obtained from the enthalpy of reaction (iii) and the experimental excitation energy of triplet CH₃N. The enthalpy of reaction (ii) is obtained from the relative energy of CH₂NH(¹A'') and CH₂NH(¹A').⁸

After photoexcitation, (i) is the predominant reaction channel, which produces ground state CH₂NH via concerted 1,2-hydrogen shift and N₂ extrusion process. Reaction (ii) needs about 35 kcal to overcome the activation barrier from the Jahn–Teller component ¹A'' of singlet CH₃N to the transition state⁸ and is energetically accessible at photolysis wavelengths from 292 nm to 325 nm. Reaction (iii) is spin-forbidden and occurs on the singlet surface in the beginning, then goes down and crosses with the triplet dissociation surface. Most of the reaction trajectories keep on going along the singlet surface, while a few of them turn to go along the triplet surface, giving the triplet fragment in result. The enthalpy for reaction (iv) is 96.6 kcal mol⁻¹, which is close to the photolysis energy. Meanwhile, the excitation of triplet state (*T*₁) is also possible, but it is expected to be a minor process. Two mechanisms are responsible for the production of CH₃N(\tilde{A}^3E). On the one hand, since it is energetically accessible at short photolysis wavelengths, channel (iv) may happen; on the other hand, the excitation of ground state CH₃N is also possible to produce an excited state CH₃N. It is difficult to distinguish these two processes in our experiment.

So far, the photodissociation processes of CH₃N₃ seem to be complex and interesting. A detailed *ab initio* investigation of low-lying excited potential surfaces and dissociation dynamics of CH₃N₃ are desired. The spin–orbit coupling as well as singlet and triplet conical intersection zone may be clarified by theoretical treatment. Further experiments such as femto-laser photolysis study would also make sure whether singlet CH₃N is a local minimum like singlet methylcarbene (CH₃CH) or just a saddle point on the potential surface. In addition, 308 nm excimer laser photolysis of CH₃N₃ may be an available CH₃N radical source though it is not as efficient as the NH source produced by photolysis of HN₃.

V. CONCLUSION

The triplet CH₃N radical is observed in the photodissociation of methylazide at wavelengths from 292 nm to 325 nm. A kinetic model considering the vibrational relaxation of

an initially produced hot radical well explains the fluorescence lifetime profile at high pressures. The photodissociation dynamics of methylazide seems more complex. The predominant channel is likely to produce CH_2NH via a concerted process as observed previously. The spin-forbidden photodissociation channel which produces a triplet CH_3N radical might involve a strong interaction between the low-lying excited singlet and triplet states of methylazide. Further experimental and *ab initio* studies upon the photodissociation dynamics of methylazide are necessary.

ACKNOWLEDGMENTS

The authors wish to thank the financial support by NSFC and by the Fok Ying Tung Education Foundation. The purchase of the equipment used in this experiment is partly supported by the Starr Foundation through the University of California at San Francisco.

- ¹E. F. V. Scriven, *Azides and Nitrenes* (Academic, New York, 1984).
- ²D. E. Milligan, *J. Chem. Phys.* **35**, 1491 (1961).
- ³C. L. Currie and B. deB. Darwent, *Can. J. Chem.* **41**, 1552 (1963).
- ⁴D. E. Milligan and M. E. Jacox, *J. Chem. Phys.* **56**, 333 (1975).
- ⁵G. O. Braathen, P. Klaeboe, C. J. Nielsen, and H. Priebe, *J. Mol. Struct.* **115**, 197 (1984).
- ⁶H. Bock and R. Dammel, *Angew. Chem. Int. Ed. Engl.* **26**, 504 (1987).
- ⁷H. Bock and R. Dammel, *J. Am. Chem. Soc.* **110**, 5261 (1988).
- ⁸C. Richards, Jr., C. Meredith, S. Kim, G. E. Quelch, and H. F. Schaefer, *J. Chem. Phys.* **100**, 481 (1994).
- ⁹M. T. Nguyen, *Chem. Phys. Lett.* **117**, 290 (1985).
- ¹⁰J. Demuynck, D. J. Fox, Y. Yamaguchi, and H. F. Schaefer, *J. Am. Chem. Soc.* **102**, 6204 (1980).
- ¹¹J. A. Pople, K. Raghavachari, M. J. Frisch, J. S. Binkley, and P. V. R. Schleyer, *J. Am. Chem. Soc.* **105**, 6389 (1983).
- ¹²H. F. Schaefer, *Acc. Chem. Res.* **12**, 288 (1979).
- ¹³E. Wasserman, G. S. Smolinsky, and W. A. Yager, *J. Am. Chem. Soc.* **86**, 3166 (1964).
- ¹⁴P. G. Carrick and P. C. Engelking, *J. Chem. Phys.* **81**, 1661 (1984).
- ¹⁵C. R. Brazier, P. G. Carrick, and P. F. Bernath, *J. Chem. Phys.* **96**, 919 (1992).
- ¹⁶E. L. Chappell and P. C. Engelking, *J. Chem. Phys.* **89**, 6007 (1988).
- ¹⁷R. F. Ferrante, *J. Chem. Phys.* **94**, 4678 (1991).
- ¹⁸H. Shang, C. Yu, L. Ying, and X. Zhao, *Chin. J. Chem. Phys.* **6**, 438 (1993).
- ¹⁹H. Shang, C. Yu, L. Ying, and X. Zhao, *Acta Phys. Chim. Sinica* **9**, 594 (1993).
- ²⁰H. Shang, C. Yu, L. Ying, and X. Zhao, *J. Chem. Phys.* **103**, 4418 (1995).
- ²¹J. D. Evanscek and K. N. Houk, *J. Phys. Chem.* **94**, 5518 (1990).
- ²²M. M. Gallo and H. F. Schaefer, *J. Phys. Chem.* **96**, 1515 (1992).
- ²³S. Khodabandeh and E. A. Carter, *J. Phys. Chem.* **97**, 4360 (1993).
- ²⁴B. Ma and H. F. Schaefer, *J. Am. Chem. Soc.* **116**, 3539 (1994).
- ²⁵D. M. Miller, P. R. Schreiner, and H. F. Schaefer, *J. Am. Chem. Soc.* **117**, 4137 (1995).
- ²⁶D. A. Modarelli and M. S. Platz, *J. Am. Chem. Soc.* **115**, 470 (1993).
- ²⁷W. D. Closson and H. G. Gray, *J. Am. Chem. Soc.* **85**, 290 (1963).
- ²⁸H. Shang, C. Yu, L. Ying, and X. Zhao, *Chem. Phys. Lett.* **236**, 318 (1995).
- ²⁹L. Ying, Y. Xia, H. Shang, X. Zhao, and Y. Tang, *Acta Phys. Chim. Sinica* **11**, 961 (1995).
- ³⁰L. D. Ziegler, *Acc. Chem. Res.* **27**, 1 (1994).
- ³¹P. J. Bruna, V. Krumbach, and S. D. Peyerimhoff, *Can. J. Chem.* **63**, 1594 (1985).
- ³²P. R. Bevington, *Data Reduction and Error Analysis for the Physical Sciences* (New York, San Francisco, 1969).
- ³³H. Shang, L. Ying, R. Gao, X. Zhao, and Y. Tang (in preparation).
- ³⁴F. Rohrer and F. Stuhl, *J. Chem. Phys.* **86**, 226 (1987).
- ³⁵B. R. Foy, M. P. Casassa, J. C. Stephenson, and D. S. King, *J. Chem. Phys.* **89**, 608 (1988); **90**, 7037 (1989); **92**, 2782 (1990).
- ³⁶F. Rohrer and F. Stuhl, *J. Chem. Phys.* **88**, 4788 (1988).
- ³⁷K.-H. Gericke and R. Theinl, *Chem. Phys. Lett.* **164**, 605 (1990).
- ³⁸K.-H. Gericke and R. Theinl, *J. Chem. Phys.* **92**, 6548 (1990).
- ³⁹J.-J. Chu, P. Marcus, and P. J. Dagdigian, *J. Chem. Phys.* **93**, 257 (1990).
- ⁴⁰K.-H. Gericke, T. Haas, M. Lock, R. Theinl, and F. J. Comes, *J. Phys. Chem.* **95**, 6104 (1991).
- ⁴¹M. H. Alexander and H.-J. Werner, *J. Chem. Phys.* **93**, 3307 (1990).
- ⁴²U. Meier and V. Staemmler, *J. Phys. Chem.* **95**, 6111 (1991).
- ⁴³L. A. Curtiss, K. Raghavachari, and J. A. Pople, *J. Chem. Phys.* **94**, 7221 (1991).
- ⁴⁴GAUSSIAN 94, Revision A.1, M. J. Frisch, G. W. Trucks, H. B. Schlegel, P. M. W. Gill, B. G. Johnson, M. A. Robb, J. R. Cheeseman, T. Keith, G. A. Petersson, J. A. Montgomery, K. Raghavachari, M. A. Al-Laham, V. G. Zakrzewski, J. V. Ortiz, J. B. Foresman, J. Cioslowski, B. B. Stefanov, A. Nanayakkara, M. Challacombe, C. Y. Peng, P. Y. Ayala, W. Chen, M. W. Wong, J. L. Andres, E. S. Replogle, R. Gomperts, R. L. Martin, D. J. Fox, J. S. Binkley, D. J. Defrees, J. Baker, J. P. Stewart, M. Head-Gordon, C. Gonzalez, and J. A. Pople, Gaussian, Inc., Pittsburgh, Pennsylvania, 1995.
- ⁴⁵L. Ying, X. Zhao, and Y. Tang (unpublished results).